

Pulses of Fast Electrons as a Tool To Synthesize Poly(acrylic acid) Nanogels. Intramolecular Cross-Linking of Linear Polymer Chains in Additive-Free Aqueous Solution

Slawomir Kadlubowski,[†] Jaroslaw Grobelny,[‡] Wielislaw Olejniczak,[‡] Michal Cichomski,[‡] and Piotr Ulanski^{*,†}

Institute of Applied Radiation Chemistry, Technical University of Lodz, Wroblewskiego 15, 93-590 Lodz, Poland, and Department of Solid State Physics, University of Lodz, Pomorska 149/153, 90-236 Lodz, Poland

Received October 28, 2002; Revised Manuscript Received January 2, 2003

ABSTRACT: Nanogels of poly(acrylic acid) have been synthesized using a new method, based on intramolecular cross-linking of linear macromolecules in aqueous solution, induced by short (a few microseconds) pulses of fast electrons. Simultaneous generation of a number of carbon-centered radicals along the polymer chain results in predominantly intramolecular recombination, with only a minor contribution of intermolecular cross-link formation and chain scission. This new method allows the synthesis of nanogels in a pure system consisting only of polymer and water, in the absence of monomers, cross-linking agents, etc. Adjusting the polymer concentration and dose of radiation, one can control the molecular weight and dimensions of nanogels. The products have been characterized by static light scattering, viscometry, and atomic force microscopy, while the nonclassical kinetics of intramolecular recombination has been followed by time-resolved spectroscopy. Nanogels of poly(acrylic acid) are much more resistant to free-radical-induced degradation than the parent linear chains.

Introduction

Microgels are internally cross-linked, small polymer structures able to swell in a suitable solvent, usually water. Research on their synthesis, properties, and applications has gained significant momentum in the past years and has been the subject of a number of reviews.^{1–5} To distinguish between microgels of various sizes that can differ by a few orders of magnitude, we use a more specific term—*nanogels*—to denote gel particles of submicrometer size. Molecular weights and dimensions of so-defined swollen nanogels are similar to these of typical single macromolecules in solution, but the presence of internal bonds results in different physicochemical properties, including fixed shape, different rheological behavior, higher resistance to degradation, and the ability to trap other molecules within their structure.

Nano- and microgels have broad actual and potential field of applications, ranging from filler materials in coating industry to biomaterials.² In the latter area, nanogels are tested to see whether they can be used for e.g. drug delivery and targeting systems,^{6–8} blocking agents for dentinal microchannels,⁹ and components of synovial fluid substitutes.¹⁰ Recently, there has been a growing interest in the synthesis and applications of stimuli-sensitive microgels.^{7,11–16}

Most of the synthetic methods used to obtain nano- and microgels are based on polymerization in emulsion, solution, or suspension.^{1–4} A multitude of techniques has been described, including for example surfactant-free emulsion polymerization,^{4,17} living anionic or free-

radical polymerization,^{18,19} and radiation-induced polymerization.²⁰ The common feature of these techniques is that the starting materials are monomers, at least in part containing two reactive (mostly vinyl) groups.

An alternative approach to the synthesis of nanogels is intramolecular cross-linking of individual macromolecules. An important advantage of this method is the absence of monomer. This is of great value when the product is intended for biomedical use, where even small quantities of residual monomer may be potentially harmful. Furthermore, intramolecular cross-linking may provide a means to obtain cross-linked structures of various molecular weight and size, including very small structures, depending on the molecular weight of the parent polymer. Such nanogels obtained from single macromolecules are interesting physical forms of polymers as they are a sort of “frozen” polymer coils of limited segmental mobility. One can also expect that a combination of intra- and intermolecular cross-linking (cf. refs 21 and 22) will provide a tool for synthesizing nanogels of independently chosen molecular weight and dimensions (various internal densities). Last but not least, intramolecular cross-linking in polymers is an interesting reaction. A number of questions regarding this process, particularly its kinetics, have not been answered yet (cf. refs 23–25).

It has been shown that intramolecular cross-linking of single chains of water-soluble polymers can be carried out by reacting them with a suitable cross-linking agent in dilute solutions.^{26,27} Recently, we have proposed an alternative method, where neither cross-linker nor any other additive is necessary.²⁴ In this approach, discussed in more detail below, a pure aqueous solution of a polymer is subjected to a short (a few microseconds) intense pulse of ionizing radiation. In this way, many radicals are generated simultaneously along each poly-

[†] Technical University of Lodz.

[‡] University of Lodz.

* Corresponding author: e-mail ulanski@mitr.p.lodz.pl.

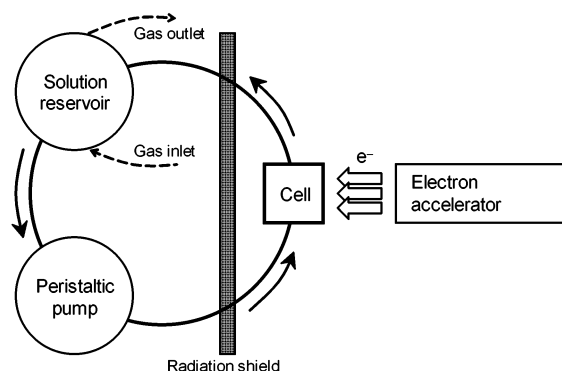


Figure 1. Schematic diagram of the pulse irradiation setup used in the synthesis of nanogels. Solid-line arrows indicate the flow of polymer solution in the closed loop.

mer chain, and their intramolecular recombination leads to the formation of nanogels. This approach has been first tested on neutral water-soluble polymers: poly(vinyl alcohol),²⁴ polyvinylpyrrolidone,²⁸ and poly(vinyl methyl ether).^{29,30}

In the present paper we report the application of this method to synthesize nanogels of poly(acrylic acid). A brief discussion of the kinetic aspects of this synthesis has been published separately.²⁵

Experimental Section

Poly(acrylic acid) (PAA, Aldrich, nominal $M_w = 2.5 \times 10^5$ Da) was purified from traces of volatile impurities (water, monomer, and solvent) by heating at 40 °C in a vacuum for 2 h. The actual M_w , as determined by multiangle laser light scattering (see below), was 5.2×10^5 Da. Solutions of PAA were prepared by overnight stirring at 50 °C. When needed, the pH was adjusted with HClO_4 (perchlorate ions are relatively radiation-resistant) or NaOH. Other chemicals were of high purity and used as received.

Water purified by the Nanopure II system (Barnstead), having specific resistivity of over 17 M Ω cm and passed through a 0.2 μm pore size filter, was used in all experiments.

Pulse irradiation (see discussion in the text below) was conducted in a setup shown schematically in Figure 1. Aqueous PAA solution (pH = 2.0, HClO_4), saturated with oxygen-free argon (saturation started 1 h before the irradiation and continued during the process), was circulating at 1 $\text{cm}^3 \text{s}^{-1}$ in a gastight, closed-loop system, passing through a quartz cell (effective volume: 0.7 cm^3) that was subjected to short pulses of fast electrons [pulse duration: 2 μs , pulse frequency: 0.5 Hz, electron energy: 6 MeV, absorbed dose of ionizing radiation per single pulse: 1.15 kGy (1 Gy = 1 J kg^{-1})], generated by an ELU-6 linear accelerator (Eksma, Russia). Knowing the parameters of the system, it was possible to set the total irradiation time so as to ensure that on average each volume element (0.7 cm^3) of the solution absorbed one shot (average absorbed dose equal to a dose in a single shot; this corresponds to the lowest doses shown in Figures 4–6) or any other desired number of shots.

The same pulse radiolysis setup was used to follow the kinetics of intramolecular cross-linking. In these experiments, a light beam from a Xe lamp was passed through the cell. The time-resolved intensity of transmitted light at a selected wavelength (SpectraPro 275 monochromator, Princeton Instruments) was measured by a fast photomultiplier (Hamamatsu) coupled to digitizing oscilloscopes. The analytical wavelength was chosen as $\lambda = 280$ nm, where both radicals **1** and **2** (cf. reaction 3) absorb light with similar extinction coefficients.³¹

The doses of ionizing radiation in pulse-irradiation synthesis and kinetic experiments were determined with ferrocyanide dosimeter.^{32–34}

Tests on the radiation-induced degradation of linear and cross-linked PAA were performed on the same setup as used in the synthesis, but the solutions were saturated with oxygen and the dose per pulse was lowered to 20 Gy. The pulse duration was 17 ns, and the doses were determined by standard thiocyanate dosimetry.³⁵

Static multiangle laser light scattering measurements were carried out on a BI-200SM goniometer (Brookhaven) with a Lexel 95E Ar ion laser ($\lambda = 514.5$ nm), at 25.0 ± 0.1 °C, in an aqueous solution of pH 10.0 (NaOH) containing 0.5 M NaClO_4 . The refractive index increment of PAA in this solvent is $dn/dc = 0.30 \text{ cm}^3 \text{g}^{-1}$.³¹ It has been assumed that cross-linking would not affect this parameter. Prior to the measurement, each sample was filtered through a 0.45 μm pore size filter (Minisart, Sartorius). Data were analyzed according to the Zimm algorithm.

Viscosities were measured on an automatic Ubbelohde viscometer AVS-310 (Schott) at 25.0 ± 0.1 °C.

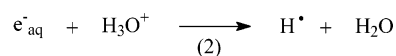
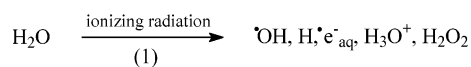
Visualization of nanogels was performed by atomic force microscopy (AFM).^{36–38} The films cast from 10% (w/v) salt-free solutions of linear PAA and nanogels were air-dried in a dust-free atmosphere at room temperature. The AFM pictures were obtained using microscope constructed in Department of Solid State Physics, University of Lodz. Pyramidally shaped silicon nitride (Si_3N_4) cantilevers manufactured by Digital Instruments, Inc., of an average radius of 20 nm were used. A beam deflection scheme with a four-quadrant photodetector allows the measurement of normal displacement. This was the way topography was imaged with molecular resolution. All measurements were done in a contact mode. The experiments were conducted at room temperature and a relative air humidity of about 60%.

Unless stated otherwise, the polymer concentrations are expressed as mol of monomer unit per dm^3 .

Results and Discussion

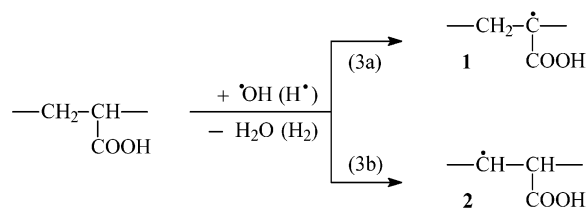
Generation of Radicals along the PAA Chain.

The action of ionizing radiation, either in the form of γ -rays or fast electrons, on polymers in dilute aqueous solutions occurs mainly through an indirect effect. Most part of the energy is absorbed by water. Ionization of water molecules and subsequent cascade of events leads on a subnanosecond time scale to the formation of reactive species: hydroxyl radicals, hydrogen atoms, and hydrated electrons (reaction 1). The initial radiation chemical yields of these species in Ar-saturated solutions are $G(\text{OH}) = 2.8 \times 10^{-7} \text{ mol J}^{-1}$, $G(\text{H}) = 0.6 \times 10^{-7} \text{ mol J}^{-1}$, and $G(\text{e}_{\text{aq}}^-) = 2.7 \times 10^{-7} \text{ mol J}^{-1}$.³⁹ At pH = 2 used in our experiments, hydrated electrons are converted, within the pulse duration, into further hydrogen atoms (reaction 2, $k = 2.3 \times 10^{10} \text{ dm}^3 \text{mol}^{-1} \text{s}^{-1}$).⁴⁰



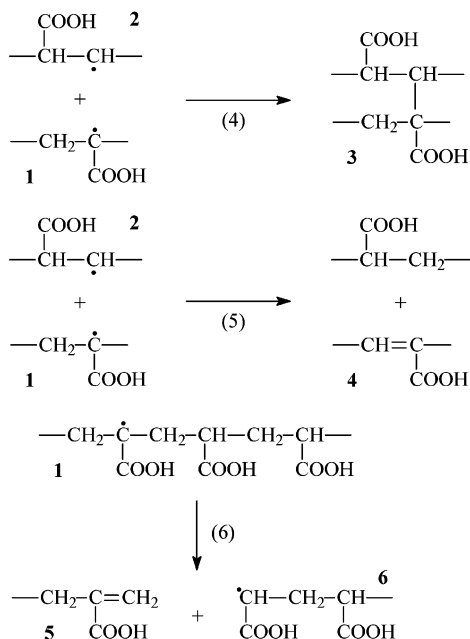
Subsequently, hydroxyl radicals and hydrogen atoms react rapidly with PAA by hydrogen abstraction (reaction 3, $k(\text{OH} + \text{PAA}) = 9.0 \times 10^7 \text{ dm}^3 \text{mol}^{-1} \text{s}^{-1}$ ⁴¹ for our sample, the value being dependent on the molecular weight, while H atoms react more slowly by an order of magnitude), and in this way polymer-derived midchain radicals **1** and **2** are formed, their initial molar ratio being ca. 1:2.³¹ In the case of low-molecular-weight carboxylic acids, hydroxyl radicals do not react with carboxylic groups.^{42–44} Similarly, no evidence of such

reactions has been found for PAA.³¹



Recombination of Radicals and Competing Reactions. The fate of the PAA-derived radicals **1** and **2** had been studied before in some detail.³¹ As can be expected, it depends strongly on pH. In neutral and alkaline solutions, where the carboxylic groups are deprotonated and there is a high density of negative charge along the chains, radicals cannot recombine easily due to the repulsive Coulombic forces. As a result, they can have a lifetime of several minutes or even hours, which is a somewhat unusual feature for simple alkyl-type radicals in aqueous solution at room temperature.^{31,45} Certainly, these are very unsuitable conditions for cross-linking. Instead, strong degradation and other side reactions are observed. On the other hand, it has been shown that at pH < 3, where the carboxylic groups are protonated, recombination of radicals becomes very fast, and therefore cross-linking dominates over scission, at least under the conditions of continuous γ -irradiation.^{31,46} Since the solubility of PAA in water decreases at pH < 1,⁴⁷ we have chosen to work at pH = 2.

Under such conditions, where the PAA-derived radicals have a relatively short lifetime, slow side processes such as for example H-shift do not show up, and the list of possible reactions of these radicals is limited to recombination, disproportionation, and chain scission (by β -fragmentation); see exemplary reactions 4–6.



The ratio of the recombination to the disproportionation occurring when two radicals approach each other is a function of their chemical structure and cannot be easily influenced. It has been shown in a study on the radicals of a PAA model compound, 2,4-dimethylglutaric acid, that ca. 45% of them decay by recombination,⁴⁴ and

this value sets the limit of the fraction of PAA radicals that will yield cross-links, irrespective on the method of their generation. The rest is “lost”, at least at this stage of gel formation.

Strictly speaking, chain scission and recombination are not competing reactions, since in the course of the former the number of radicals in the system does not change. In other words, each radical that undergoes fragmentation yields another radical that will finally recombine (or disproportionate). Thus, scission does not deplete the substrates available for recombination. But, of course, the average number of scission events occurring per a recombination event is of major importance to the final effect of the whole process and to the properties of the product—if the scission/recombination ratio is too high, no gel will be formed. In the case of PAA it seems that degradation cannot be totally avoided, but its yield can be kept low. Fortunately, as will be shown below, in the course of intramolecular cross-linking the influence of degradation diminishes gradually during the process.

Reaction Conditions Promoting Inter- or Intramolecular Recombination. Recombination may occur either between two radicals localized on separate macromolecules or between two radicals within the same chain. The first of these processes leads to intermolecular cross-linking and increase in average molecular weight and finally may result in the formation of macroscopic (“wall-to-wall”) gels. This reaction is the base of radiation technologies used to produce hydrogel materials on an industrial scale, mostly in the biomedical industry.^{48–50} Intramolecular recombination does not influence molecular weight but, by the formation of new C–C bonds between the formerly independent chain segments, yields nanogels.

The main parameter influencing the competition between inter- and intramolecular recombination in dilute polymer solutions (i.e., when coils are separated from each other) is the average number of radicals present at each macromolecule at the same time.²³ If this number, under the given synthesis conditions, is much smaller than 1, there is only a meager chance that a radical will find a reaction partner within the same chain. In such cases, recombination is only possible between radicals localized on two separate macromolecules. On the other hand, when there are tens of radicals present along each chain, the probability of intramolecular encounters and reactions is higher than that of intermolecular ones. The latter processes are relatively slow, since for them to occur two large entities—polymer coils—have to diffuse toward each other.

In the case of the radiation-induced radical formation, these two opposite conditions, i.e., a very low or very high number of radicals per chain, can be fulfilled by means of a proper choice of irradiation conditions (Figure 2). Continuous irradiation at a relatively low dose rate, such as typical irradiation with γ -rays from isotope sources, leads to a steady-state concentration of polymer radicals on the order of 10^{-7} M. When the concentration of polymer coils is significantly higher than the above value (this condition is usually easily fulfilled), the average number of radicals per chain is much lower than unity, and intermolecular cross-linking is observed. To promote intramolecular cross-linking, short, intense pulses of radiation can be employed, such as pulses of fast electrons from an accelerator, generat-

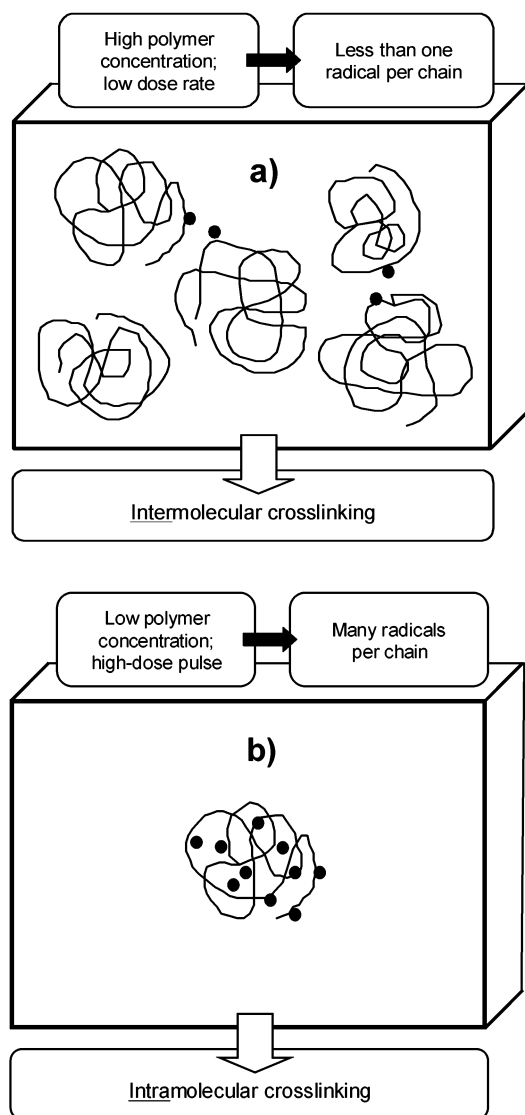


Figure 2. Irradiation conditions promoting: (a) inter- and (b) intramolecular recombination of polymer-derived radicals in solution.

ing radical concentrations on the order of 10^{-4} – 10^{-3} M. If the concentration of polymer coils is low (that is to say, 10^{-6} – 10^{-4} M), many radicals are generated on each macromolecule (typically many tens or even over a hundred), and the conditions for intramolecular recombination are fulfilled. Certainly, this does not mean that intermolecular reactions are totally eliminated in such a case; some coils may come into contact before all the radicals decay, and if there is an uneven number of radicals on a chain, at least one of them must finally find a reaction partner at a neighboring macromolecule.

In this work we have used PAA concentrations in the range 10–25 mM monomer units. This corresponds to 0.72–1.80 g/dm³ (which is lower than the coil overlapping concentration estimated for our PAA sample at pH 2 as ca. 10 g/dm³) and to approximately $(3\text{--}7) \times 10^{-6}$ M polymer coils.

Kinetics. The progress of intramolecular recombination initialized by pulse irradiation of a polymer solution can be followed, and easily distinguished from intermolecular reactions, by kinetic measurements or by analysis of the products formed. Since the kinetic analysis of intramolecular recombination of radicals has been

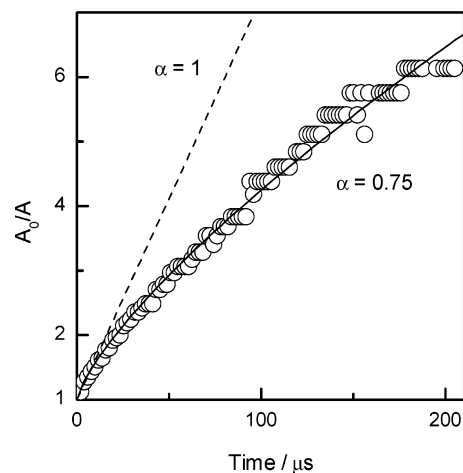


Figure 3. Decay kinetics of PAA-derived radicals generated by high-dose pulse irradiation. Absorbance of radicals (A) at 280 nm related to their initial absorbance (A_0) plotted vs time after pulse in the coordinates of second-order kinetics: \circ , typical set of experimental data; solid line, fit with eq 1; broken line, theoretical decay curve for classical second-order reaction with time-independent rate constant. [PAA] = 17.5 mM, pH 2, dose per pulse 1.15 kGy, pulse duration 2 μ s, Ar-saturated aqueous solution.

already presented for a number of water-soluble polymers,^{23,24,29,51,52} including PAA,²⁵ we will limit here the presentation and discussion of kinetic data to the most essential facts. Recombination of two polymer-derived radicals localized at separate macromolecules can be approximated as a predominantly diffusion-controlled process involving two separate, independent entities and following the Smoluchowski equation, thus adhering to classical second-order kinetics. This is no longer the case when we move to intramolecular recombination. There, the kinetics is governed by the segmental mobility within a polymer chain. The reacting entities are no longer independent. The time scale and energy barrier of their mutual approach depend on their absolute and relative locations along the chain; therefore, the process cannot be described by a single value of activation energy, but by its distribution. Moreover, it has been postulated that the formation of new bonds between the segments makes them less flexible, thus reducing segmental mobility in the course of the reaction. Therefore, the decay kinetics of the radicals deviates strongly from the second-order pattern. This kinetic feature can be employed to detect the nature of dominating reaction in a given system, i.e., to find out whether inter- or intramolecular recombination prevails. The presence of disproportionation does not influence the kinetics, since the rate-determining steps (approach of two radicals into reaction distance) in the case of disproportionation and recombination are identical.

Figure 3 shows typical decay kinetics of PAA-derived radicals under the pulse-irradiation conditions used in the synthesis of PAA nanogels, in coordinates corresponding to classical second-order reaction. The experimental points do not follow a straight line. Instead, the momentary rate constant (the slope) decreases during the reaction. This is a typical feature for intramolecular recombination.

To quantify the deviation from classical kinetics, one can fit kinetic data with a dispersive kinetics model (eq 1)⁵³

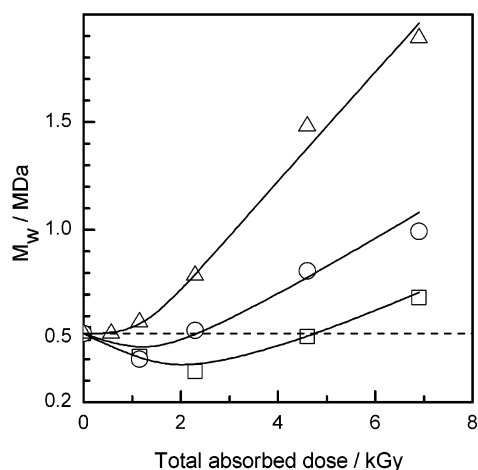


Figure 4. Changes in the weight-average molecular weight of PAA molecules in the course of nanogel synthesis as a function of total absorbed dose (1.15 kGy corresponds to a single pulse) for samples of various PAA concentrations: \square , 10 mM; \circ , 17.5 mM; \triangle , 25 mM; irradiated in Ar-saturated aqueous solutions, pH 2.

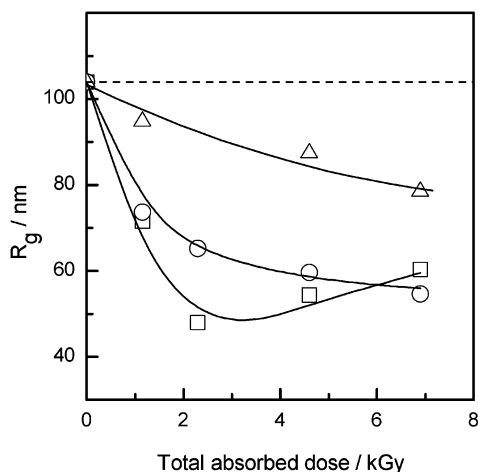


Figure 5. Changes in the radius of gyration of PAA molecules in the course of nanogel synthesis as a function of total absorbed dose (1.15 kGy corresponds to a single pulse) for samples of various PAA concentrations: \square , 10 mM; \circ , 17.5 mM; \triangle , 25 mM; irradiated in Ar-saturated aqueous solutions, pH 2. Radii of gyration measured at 25.0 °C in aqueous 0.5 M NaClO₄, pH 10.

$$k(t) = Bt^{\alpha-1} \quad (1)$$

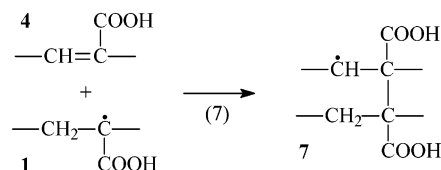
where k is the time-dependent rate constant, t is reaction time, and B and α are parameters. The parameter α can be used as a measurement of the deviation from the classical second-order kinetics. For $\alpha = 1$, eq 1 yields a "normal", time-independent rate constant (see the broken line in Figure 3). The lower the α value, the more pronounced is the nonclassical character of the reaction. Typically, values between 0.4 and 0.8 are observed for dominating intramolecular recombination. The α values measured in the current system under the conditions of our syntheses are within this range.

Product Analysis. Figures 4 and 5 illustrate the changes in weight-average molecular weight and radius of gyration of PAA subjected to pulse irradiation in solutions of various concentrations as a function of total absorbed dose.

The data clearly indicate that, regardless of the polymer concentration, at high doses we obtain strongly

internally cross-linked nanogels which, in comparison with the starting macromolecules, have higher molecular weight but at the same time significantly lower dimensions. While the main reason for the increase in molecular weight is the intermolecular cross-linking occurring in the system with very low yields (see below) in parallel to intramolecular recombination, the latter process is the dominant reason for the reduction in coil dimensions.

At the first stage of irradiation (first pulse corresponding to the dose of 1.15 kGy), for low PAA concentrations there is some decrease in the molecular weight, which is evidence of the fact that the balance between intermolecular cross-linking and chain scission is initially shifted toward the latter reaction. However, very soon this tendency is reversed. The most probable reason is that internal cross-links that have been already formed make the structure less prone to losing fragments as a result of degradation. In other words, a chain segment of a nanogel is bound to other segments with more than one joint; thus, if a chain break occurs in this segment, it does not cause its detachment from the rest of the molecule (see more detailed data and discussion below). Moreover, the nanogels, due to their reduced dimensions compared to the initial coils, have higher translational mobility; thus, the rate of their mutual encounters leading to intermolecular cross-linking should increase. (This effect is, however, counterbalanced to a certain extent by the reduced reaction radii, making the necessary diffusion distance longer.) Another factor that may contribute to the increase in efficiency of cross-linking (both inter- and intramolecular) in the course of the process is the accumulation of double bonds that are formed as a result of disproportionation events (cf. reaction 5). Addition of a polymer radical to such a bond (reaction 7) creates the desired cross-link and leaves behind another polymer radical, capable of participating in further cross-linking steps.



The higher the polymer concentration, the higher the yield of intermolecular cross-linking (due to the lower number of radicals per chain and closer distance between the coils), and therefore for 25 mM PAA there is no initial decrease in M_w . Finally, we obtain products of molecular weight higher than the molecular weight of the parent chains, but which have much smaller radii of gyration. Such a tight conformation, which is more densely packed than the starting coils of linear macromolecules, is a typical feature of internally cross-linked chains.^{2,27} Reduction in dimensions despite the increase in M_w is also evidenced by a pronounced decrease in intrinsic viscosity (Figure 6).

Only in the 10 mM solution is no further decrease of radius of gyration observed after a certain dose. It should be noted that intramolecular cross-linking is most effective at the lowest concentration (highest number of radicals per chain at a given dose per pulse), and perhaps a stage of tightly cross-linked structure is reached. (The coil density is some 10 times higher than

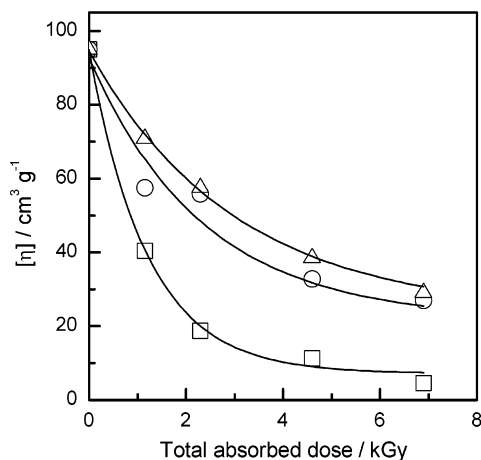


Figure 6. Changes in intrinsic viscosity of PAA solutions in the course of nanogel synthesis as a function of total absorbed dose (1.15 kGy corresponds to a single pulse) for samples irradiated in Ar-saturated aqueous solutions, pH 2, at various PAA concentrations: \square , 10 mM; \circ , 17.5 mM; \triangle , 25 mM. Viscosity measured at 25.0 °C in aqueous 0.5 M NaClO₄, pH 10.

in the initial free coil.) The possibility that a further intramolecular recombination occurs is reduced because of the relatively rigid structure and limited mobility of the chain segments. Probably at this stage intermolecular cross-linking starts to play a more significant role, so that some fraction of the already formed nanogels becomes subsequently linked together. This effect is, however, not very pronounced, since no increase in viscosity is observed. One should bear in mind that the R_g values resulting from light scattering are z -averages that are very sensitive to the presence of even tiny fractions of aggregates (while viscosity is not). This seems to be the reason why there is an apparent discrepancy between the trends in R_g and viscosity data for the 10 mM solution within the discussed dose range.

An important message from the data in Figure 4 is that under these conditions intermolecular cross-linking is indeed a minor process compared to intramolecular recombination. Let us estimate the maximum yield of intermolecular cross-linking in our system. In a situation where cross-linking and scission occur side by side, using the M_w vs dose plot, one can directly calculate only the difference of yields, precisely the value of $G(x, \text{inter}) - 4G(s)$ (cf. refs 54 and 55). At the highest slope in the M_w vs dose plot (data for 25 mM PAA between 1.15 and 6.9 kGy where cross-linking clearly dominates over scission), this difference is ca. $2 \times 10^{-10} \text{ mol J}^{-1}$. Now one has to assume the scission frequency compared to cross-linking events. Since the slope is positive, $G(x, \text{inter}) > 4G(s)$, there must be more than four intermolecular cross-linking events per one scission event. Even if we assume that cross-linking only slightly prevails over scission and there are five cross-links per one scission event, we arrive at no more than $G(x, \text{inter}) = 1 \times 10^{-9} \text{ mol J}^{-1}$ of intermolecular cross-links being formed. This value should be compared with the total yield of recombination events in the system. If we have the initial yield of OH and H equal $6 \times 10^{-7} \text{ mol J}^{-1}$ and we assume 50% loss of OH (and H) radicals due to self-combination [$k(\text{OH} + \text{OH}) = 5.5 \times 10^9 \text{ dm}^3 \text{ mol}^{-1} \text{ s}^{-1}$]⁴⁰ and a 45% fraction of recombination reactions (see above) as well as that two radicals are used to form one cross-link, the total yield of recombination can be estimated at $G(x, \text{total}) = 7 \times 10^{-8} \text{ mol J}^{-1}$. The real

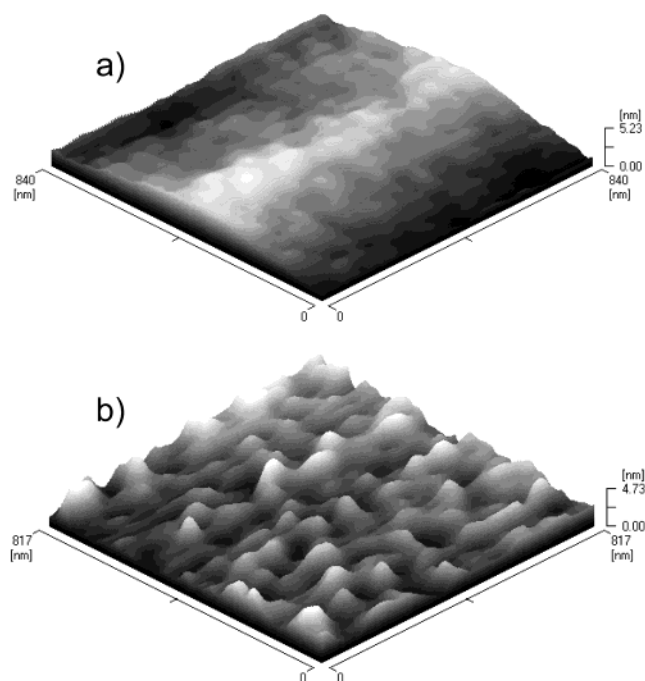


Figure 7. Atomic force microscopy pictures of dry films cast from 10% (w/v) aqueous solution of (a) linear PAA and (b) nanogels of PAA (obtained by irradiation of 17.5 mM PAA solution at pH 2 with a total dose of 2 kGy).

value is probably even higher than this estimate, because in the above calculation of $G(x, \text{total})$ the additional cross-links formed in reaction 7 were not taken into consideration. Since the yield of intermolecular cross-linking constitutes less than 2% of the total recombination yield, over 98% of the recombination events must have occurred in the intramolecular way.

To visualize the synthesized structures, AFM pictures were taken of dry films cast from solutions of linear PAA and nanogels (Figure 7, a and b, respectively). Despite the deswelling and shrinking of the gels due to the loss of water, the spherical contours of individual nanogel particles can be clearly seen on the surface of the film, in contrast to the flat surface of the film cast from linear PAA. Similar results were reported by Kim et al.,⁵⁶ where a solid PAA film was formed on a poly(vinyl sulfate) layer. Films cast from salt-free solutions had relatively smooth surfaces, while PAA chains of strongly coiled conformation formed in the presence of salt were characterized by a much rougher surface.

Swelling Properties. PAA nanogels bearing many carboxylic groups are expected to undergo expansion and contraction with changes in pH, albeit the magnitude of changes in their dimensions should be different than in the case of free linear chains. Such an effect is indeed observed. The data shown in Figure 8 illustrate the pH dependence of viscosity for the solutions of PAA molecules in the linear and nanogels forms at identical concentrations. The average molecular weight of the nanogel sample used in these experiments matched that of the linear sample. The viscosity of 5 mM nanogel solution at pH 2 was chosen as a relative unit in Figures 8 and 9. At pH 2, the solution of linear PAA has a viscosity 1.8 times higher than the nanogel solution. The expansion of the linear PAA accompanying the change of conformation from a coil at low pH to a rodlike structure in the alkaline region results in a ca. 32-fold increase in the solution viscosity, while in the case of

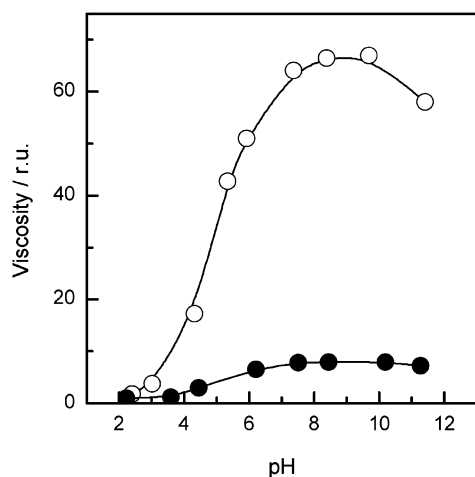


Figure 8. Relative viscosity of 5 mM PAA solutions as a function of pH for (○) linear chains and (●) nanogels of comparable weight-average molecular weight (ca. 5×10^5 Da). One unit corresponds to the viscosity of the salt-free nanogel solution at pH 2 (solution of linear chains at pH 2 has a viscosity of 1.8 units).

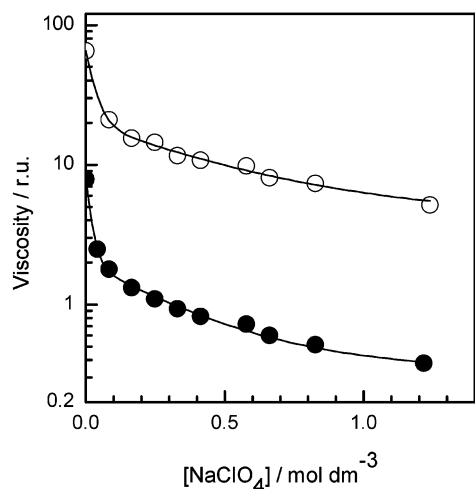


Figure 9. Relative viscosity of 5 mM PAA solutions at pH 10 as a function of salt concentration for (○) linear chains and (●) nanogels of comparable weight-average molecular weight (ca. 5×10^5 Da). One unit corresponds to the viscosity of the salt-free nanogel solution at pH 2.

nanogels the expansion factor is only ca. 7. As a result, at the pH corresponding to the highest magnitude of electrostatic repulsive forces between the chain segments, the viscosity of a solution of the expanded linear chains is 8-fold higher than the viscosity of nanogels having the same average molecular weight.

Figure 9 illustrates the contraction behavior of both samples induced by adding a simple electrolyte at pH 10. Although the salt concentration dependencies of viscosity have similar shapes for both linear and internally cross-linked chains, quantitative data indicate that nanogels are more susceptible to salt-induced collapse. Already at 0.3 M NaClO_4 the hydrodynamic dimensions of nanogels drop below the initial value corresponding to salt-free solution of pH 2 (i.e., below the viscosity of 1 relative unit, see above), while for linear chains even 1.2 M NaClO_4 is not enough to bring the viscosity back to the initial level. Similar differences in the swelling properties of linear and internally cross-linked macromolecules in response to changes in salt concentration

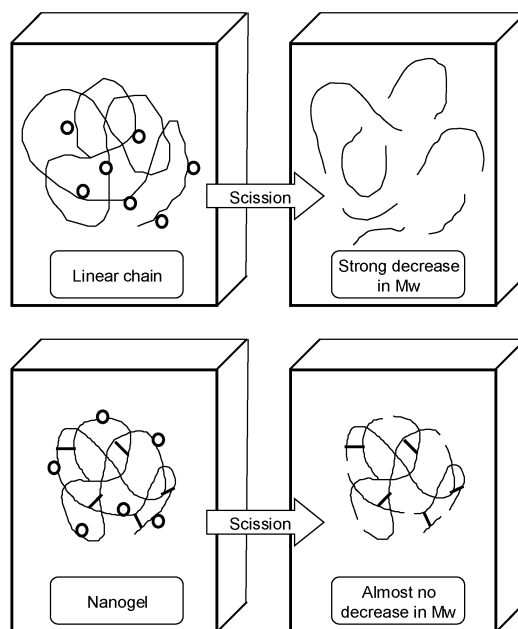


Figure 10. Scheme illustrating the impact of radical-induced chain scission of linear chains and nanogels in the presence of oxygen on their average molecular weight. ○ denotes a scission-initiating peroxy radical.

have been reported for nanogels of a cationic polyelectrolyte, poly(allylamine).²⁶

Degradation Resistance. One of the most valuable properties of nanogels is their enhanced resistance against degradation. This effect is illustrated in Figure 10. As a result of any intense or long-lasting stimulus inducing chain breakage (a mechanochemical action, ultrasound, the formation of peroxy radicals along the chain, etc.), a linear macromolecule is easily degraded to short fragments. The same number of chain breaks formed in a nanogel may cause no or very little fragmentation, since the chain segments are linked together in many points and will not fall apart as a result of a single chain break.

To verify this assumption, aqueous solutions of linear chains and nanogels of PAA were subjected to the action of ionizing radiation in the presence of oxygen. Under such conditions, no cross-linking takes place in the system.^{44,57} Initially formed carbon-centered radicals **1** and **2** are rapidly converted into the corresponding peroxy radicals, which in turn initiate processes leading to chain scission. As the concentrations of linear and cross-linked chains of similar average molecular weight were identical, the yield of scission events should be equal for both samples. However, the changes in molecular weight (Figure 11) and in the radius of gyration (Figure 12) in the case of linear and nanogel PAA show striking differences. While linear PAA is easily degraded even at relatively low doses, which is clear from the parallel decrease in M_w and R_g , nanogels, within the same dose range, seem to remain intact.

Preliminary studies of ultrasound-induced degradation of linear and internally cross-linked polymer chains also clearly indicate that nanogel structures are characterized by a much higher resistance.⁵⁸

High degradation resistance shown by nanogels may be important for some potential medical applications. An example may be using polymer drugs to enhance the viscoelastic performance of synovial fluid.⁵⁹ These macromolecules are subjected to mechanochemical stress

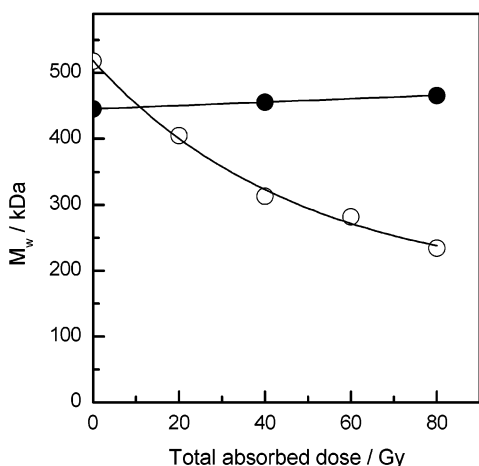


Figure 11. Free-radical-induced degradation of PAA in O_2 -saturated aqueous solutions, pH 2, initiated by pulse irradiation (pulse duration 17 ns, dose per pulse 20 Gy). Changes in the weight-average molecular weight as a function of total absorbed dose: \circ , linear chains; \bullet , nanogels (obtained by pulse irradiation of Ar-saturated 10 mM PAA solution, pH 2, with a total dose of 4.4 kGy). Polymer concentration in both samples: 10 mM.

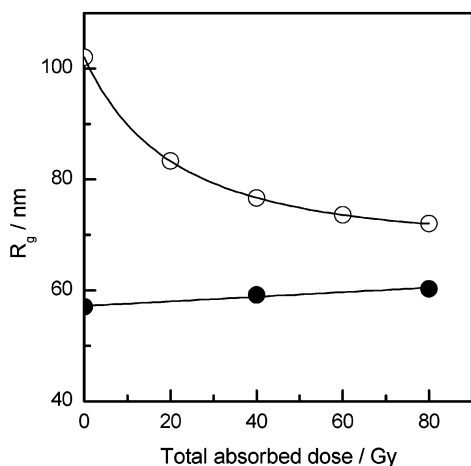


Figure 12. Free-radical-induced degradation of PAA in O_2 -saturated aqueous solutions, pH 2, initiated by pulse irradiation (pulse duration 17 ns, dose per pulse 20 Gy). Changes in the radius of gyration (determined in aqueous 0.5 M $NaClO_4$, pH 10) as a function of total absorbed dose: \circ , linear chains; \bullet , nanogels (obtained by pulse irradiation of Ar-saturated 10 mM PAA solution, pH 2, with a total dose of 4.4 kGy). Polymer concentration in both samples: 10 mM.

and abnormally high radical concentrations. It has been shown that under such conditions internally cross-linked macromolecules perform better than the corresponding linear ones.⁶⁰

Conclusions

On the example of poly(acrylic acid) we have shown that subjecting linear polymer chains in solution to short, intense pulses of ionizing radiation is an efficient tool for inducing intramolecular cross-linking of individual macromolecules, leading to the formation of nanogels.

When many carbon-centered radicals are generated simultaneously along each PAA chain in dilute solution, their recombination occurs mainly within a single chain, with only minor contributions of intermolecular recombination and chain scission.

The intramolecular recombination of the radicals derived from PAA is governed by segmental movements and, in contrast to most intermolecular radical–radical recombination reactions, does not follow classical second-order kinetics.

The average molecular weight and dimensions of the products may be controlled by changing the initial polymer concentration and the dose absorbed by the sample.

The method allows synthesizing nanogels in a pure polymer–water system, eliminating the use of monomers, cross-linking agents, or other auxiliary substances. Therefore, it seems to be especially suitable for synthesizing polymeric nanogels for biomedical purposes.

As expected, the pH and ionic strength response of PAA nanogels are different than those of linear macromolecules. Constraints imposed by the intramolecular linkages hamper the expansion of nanogels with increasing deprotonation of carboxylic groups. By contrast, nanogels are more susceptible to the collapse caused by charge screening effects upon addition of salt.

Nanogels of poly(acrylic acid) are much more resistant to free-radical-induced degradation than the parent linear macromolecules.

Acknowledgment. The authors thank Professor Janusz M. Rosiak for valuable discussions and the LINAC staff for their skillful technical assistance. This work was in part financed by the State Committee for Scientific Research, Poland (Grants No. 3 T09B 053 19, 4 T09A 128 22).

References and Notes

- (1) Antonietti, M. *Angew. Chem.* **1988**, *100*, 1813–1817.
- (2) Funke, W.; Okay, O.; Joos-Müller, B. *Adv. Polym. Sci.* **1998**, *136*, 139–234.
- (3) Graham, N. B.; Cameron, A. *Pure Appl. Chem.* **1998**, *70*, 1271–1275.
- (4) Saunders, B. R.; Vincent, B. *Adv. Colloid Polym. Sci.* **1999**, *80*, 1–25.
- (5) Tobita, H.; Kumagai, M.; Aoyagi, N. *Polymer* **2000**, *41*, 481–487.
- (6) Langer, R. *Nature (London)* **1998**, *392* (Suppl.), 5–10.
- (7) Pelton, R. *Adv. Colloid Interface Sci.* **2000**, *85*, 1–33.
- (8) Vinogradov, S.; Batrakova, E.; Kabanov, A. *Colloids Surf. B: Biointerfaces* **1999**, *16*, 291–304.
- (9) Linden, L.-A. Native and synthetic ionotropic hydrogels for use in dental care. In *Proceedings of the 5th International Symposium "Chemistry Forum 99"*; Jarosz, M., Ed.; Warsaw University of Technology: Warsaw, 1999; pp 65–68.
- (10) Ulanski, P.; Janik, I.; Kadlubowski, S.; Kozicki, M.; Kujawa, P.; Pietrzak, M.; Stasica, P.; Rosiak, J. M. *Polym. Adv. Technol.*, **2002**, *13*, 951–959.
- (11) Zhou, S.; Chu, B. *J. Phys. Chem. B* **1998**, *102*, 1364–1371.
- (12) Senff, H.; Richtering, W. *Colloid Polym. Sci.* **2000**, *278*, 830–840.
- (13) Senff, H.; Richtering, W. *J. Chem. Phys.* **1999**, *111*, 1705–1711.
- (14) Morris, G. E.; Vincent, B.; Snowden, M. J. *Prog. Colloid Polym. Sci.* **1997**, *105*, 16–22.
- (15) Daly, E.; Saunders, B. R. *Langmuir* **2000**, 5546–5552.
- (16) Daly, E.; Saunders, B. R. *Phys. Chem. Chem. Phys.* **2000**, *2*, 3187–3193.
- (17) Bartsch, E.; Kirsch, S.; Lindner, P.; Scherer, T.; Staelen, S. *Ber. Bunsen-Ges. Phys. Chem.* **1998**, *102*, 1597–1602.
- (18) Saito, R.; Ishizu, K. *Polymer* **1997**, *38*, 225–229.
- (19) Abrol, S.; Kambouris, P. A.; Looney, M. G.; Solomon, D. H. *Macromol. Rapid Commun.* **1997**, *18*, 755–760.
- (20) Yoshida, M.; Asano, M.; Kaetsu, I.; Morita, Y. *Yakuzaigaku* **1982**, *42*, 137–145.
- (21) Wang, B.; Mukataka, S.; Kodama, M.; Kokufuta, E. *Langmuir* **1997**, *13*, 6108–6114.
- (22) Wang, B.; Mukataka, S.; Kokufuta, E.; Ogiso, M.; Kodama, M. *J. Polym. Sci., Part B: Polym. Phys.* **2000**, *38*, 214–221.

- (23) Ulanski, P.; Zainuddin; Rosiak, J. M. *Radiat. Phys. Chem.* **1995**, *46*, 917–920.
- (24) Ulanski, P.; Janik, I.; Rosiak, J. M. *Radiat. Phys. Chem.* **1998**, *52*, 289–294.
- (25) Ulanski, P.; Kadlubowski, S.; Rosiak, J. M. *Radiat. Phys. Chem.* **2002**, *63*, 533–537.
- (26) Frank, M.; Burchard, W. *Makromol. Chem., Rapid Commun.* **1991**, *12*, 645–652.
- (27) Brasch, U.; Burchard, W. *Macromol. Chem. Phys.* **1996**, *197*, 223–235.
- (28) Ulanski, P.; Rosiak, J. M. *Nucl. Instrum. Methods Phys. Res. B* **1999**, *151*, 356–360.
- (29) Sabharwal, S.; Mohan, H.; Bhardwaj, Y. K.; Majali, A. B. *Radiat. Phys. Chem.* **1999**, *54*, 643–653.
- (30) Arndt, K.-F.; Schmidt, T.; Reichelt, R. *Polymer* **2001**, *42*, 6785–6791.
- (31) Ulanski, P.; Bothe, E.; Hildenbrand, K.; Rosiak, J. M.; von Sonntag, C. *J. Chem. Soc., Perkin Trans. 2* **1996**, 13–22.
- (32) Rabani, J.; Matheson, M. S. *J. Phys. Chem.* **1966**, *70*, 761–769.
- (33) Broszkiewicz, R. *Chemical Methods of Dosimetry of Ionizing Radiation*; WNT: Warsaw, 1971.
- (34) Schuler, R. H.; Hartzell, A. L.; Behar, B. *J. Phys. Chem.* **1981**, *85*, 192–199.
- (35) Buxton, G. V.; Stuart, C. R. *J. Chem. Soc., Faraday Trans.* **1995**, *91*, 279–281.
- (36) Binning, G.; Quate, C. F.; Gerber, C. *Phys. Rev. Lett.* **1986**, *56*, 530.
- (37) *Modern Tribology Handbook*; CRC Press: Boca Raton, FL, 2001; Vols. I, II.
- (38) Feldman, K.; Fritz, M.; Hahner, G.; Marti, A.; Spencer, N. D. *Tribol. Int.* **1998**, *31*, 99–105.
- (39) von Sonntag, C. *The Chemical Basis of Radiation Biology*; Taylor and Francis: London, 1987.
- (40) Buxton, G. V.; Greenstock, C. L.; Helman, W. P.; Ross, A. B. *J. Phys. Chem. Ref. Data* **1988**, *17*, 513–886.
- (41) Ulanski, P.; Rosiak, J. M. *J. Radioanal. Nucl. Chem. (Lett.)* **1994**, *186*, 315–324.
- (42) Neta, P.; Simic, M.; Hayon, E. *J. Phys. Chem.* **1969**, *73*, 4207–4213.
- (43) Schuchmann, M. N.; Zegota, H.; von Sonntag, C. *Z. Naturforsch.* **1985**, *40B*, 215–221.
- (44) Ulanski, P.; Bothe, E.; Rosiak, J. M.; von Sonntag, C. *J. Chem. Soc., Perkin Trans. 2* **1996**, 5–12.
- (45) Ulanski, P.; Bothe, E.; Hildenbrand, K.; von Sonntag, C.; Rosiak, J. M. *Nukleonika* **1997**, *42*, 425–436.
- (46) Buchanan, K. J.; Hird, B.; Letcher, T. M. *Polym. Bull. (Berlin)* **1986**, *15*, 325–332.
- (47) Molyneux, P. *Water-Soluble Synthetic Polymers. Properties and Applications*; CRC Press: Boca Raton, FL, 1987.
- (48) Rosiak, J. M. Hydrogel Dressings HDR. In *Radiation Effects on Polymers*; Clough, R. C., Shalaby, S. W., Eds.; American Chemical Society: Washington, DC, 1991; Vol. 475, pp 271–299.
- (49) Rosiak, J. M.; Ulanski, P.; Pajewski, L. A.; Yoshii, F.; Makuuchi, K. *Radiat. Phys. Chem.* **1995**, *46*, 161–168.
- (50) Rosiak, J. M.; Ulanski, P. *Radiat. Phys. Chem.* **1999**, *55*, 139–151.
- (51) Raap, I. A.; Gröllmann, U. *Macromol. Chem.* **1983**, *184*, 123–134.
- (52) Ulanski, P.; Bothe, E.; Rosiak, J. M.; von Sonntag, C. *Macromol. Chem. Phys.* **1994**, *195*, 1443–1461.
- (53) Plonka, A. *Prog. React. Kinet.* **1991**, *16*, 157–333.
- (54) Charlesby, A. *Atomic Radiation and Polymers*; Pergamon Press: Oxford, 1960.
- (55) Schnabel, W. *Polymer Degradation. Principles and Practical Applications*; Hanser: München, 1981.
- (56) Kim, D. K.; Han, S. W.; Kim, C. H.; Hong, J. D.; Kim, K. *Thin Solid Films* **1999**, *350*, 153–160.
- (57) Ulanski, P.; Bothe, E.; Hildenbrand, K.; Rosiak, J. M.; von Sonntag, C. *J. Chem. Soc., Perkin Trans. 2* **1996**, 23–28.
- (58) Kadlubowski, S.; Ulanski, P., unpublished data.
- (59) Balazs, E. A. L. Hyaluronan, its cross-linked derivative-Hylan- and their medical applications. In *Cellulosics Utilization*; Inagaki, H. P., Ed.; Elsevier Applied Science: London, 1989; pp 233–241.
- (60) Al-Assaf, S.; Phillips, G. O.; Deeble, D. J.; Parsons, B.; Starnes, H.; von Sonntag, C. *Radiat. Phys. Chem.* **1995**, *46*, 207–217.

MA021628S